Simultaneous High-Speed Recording of Sonoluminescence and Bubble Dynamics in Multibubble Fields

Carlos Cairós and Robert Mettin*
Christian Doppler Laboratory for Cavitation and Micro-Erosion, Drittes Physikalisches Institut, Georg-August-Universität Göttingen, Friedrich-Hund-Platz 1, 37077 Göttingen, Germany
(Received 26 May 2016; revised manuscript received 19 September 2016; published 8 February 2017)

Multibubble sonoluminescence (MBSL) is the emission of light from imploding cavitation bubbles in dense ensembles or clouds. We demonstrate a technique of high-speed recording that allows imaging of bubble oscillations and motion together with emitted light flashes in a nonstationary multibubble environment. Hereby a definite experimental identification of light emitting individual bubbles, as well as details of their collapse dynamics can be obtained. For the extremely bright MBSL of acoustic cavitation in xenon saturated phosphoric acid, we are able to explore effects of bubble translation, deformation, and interaction on MBSL activity. The recordings with up to 0.5 million frames per second show that few and only the largest bubbles in the fields are flashing brightly, and that emission often occurs repetitively. Bubble collisions can lead to coalescence and the start or intensification of the emission, but also to its termination via instabilities and splitting. Bubbles that develop a liquid jet during collapse can flash intensely, but stronger jetting gradually reduces the emissions. Estimates of MBSL collapse temperature peaks are possible by numerical fits of transient bubble dynamics, in one case yielding 38 000 K.

DOI: 10.1103/PhysRevLett.118.064301

Intense ultrasonic fields in liquids can cause light emission and chemical reactions, which was discovered more than 80 years ago [1,2]. The phenomena are still named after the acoustic excitation, i.e., sonoluminescence [3,4] (SL) and sonochemistry [5,6], although it became clear soon after the discovery that cavitation bubbles [7] are responsible. The reason for the extreme conditions that lead to chemistry and visible light in an otherwise "cold" bubble has been found in the energy focusing by the strong collapse, and a considerable amount of experimental and theoretical work on SL has been published in the meantime. It is remarkable that in spite of decades of research, the definite identification of the dynamics of light emitting bubbles in acoustic cavitation fields is to a good part still an open question. This is due to the fast temporal and small spatial scales involved, the typically low amount of radiated photons, and, as well, to the random nature of cavitation events. Thus, up to now, experimental investigations of SL bubble dynamics strongly rely on reproducibility or stationarity of the bubble oscillations. In particular, repeatable optical seeding [8–10] and acoustic trapping of collapsing bubbles [11–13] have allowed for a direct and detailed investigation of individual light producing bubbles. Notably, acoustic bubble trapping has boosted research efforts, and the emission from such "levitated" bubbles is termed now single-bubble sonoluminescence (SBSL). At the same time, the transferability of results from a single stationary bubble to multibubble systems has naturally been questioned, and the potential differences between trapped bubbles and those in a typical acoustic cavitation environment are still under debate. Optical emission spectra of SBSL can be significantly different from spectra of multibubble sonoluminescence (MBSL) [14]: SBSL typically shows a featureless broadband continuum, while MBSL usually exhibits clear emission lines from gas and/or liquid components, also of nonvolatile ones [15,16]. It has been suggested to explain this by bubble deformations due to instabilities, motion, or mutual bubble interactions that cause nonspherical collapse scenarios in the multibubble environments. Several observations support this idea, for instance, the appearance of emission lines for moving bubbles in traps [17,18] and in special MBSL setups with separated emission colors [19,20]. Nonetheless, the dynamics of individual bubbles in acoustic cavitation multibubble fields apparently have never been directly observed simultaneously with the process of light emission. This is particularly important since the composition of a multibubble field is inhomogeneous [21,22], and it is not clear *a priori* from which types of bubbles and under which conditions an overall MBSL signal origins. Here we demonstrate that it is possible to image at the same time bubble dynamics (oscillation and motion) and emitted light flashes with up to 0.5×10^6 frames per second. Our technique uses a sensitive high-speed camera with magnifying optics that is able to register the SL emissions with sufficient contrast against a weakly and continuously illuminated background. This allows us to connect bubble dynamics with light emission in detail on various scales, and to judge the brightness of emitting bubbles above a certain light detection threshold. We obtain information on the relative number of brightly flashing bubbles, their radius-time dynamics and translational motion, start and end of intense SL activity, the influence of shape deformations and of bubble interactions. Apart from the deeper insight into MBSL systems, the observations serve as new benchmark data for models of bubble dynamics and SL generation.

The experiments are realized in two different setups (*A* at 36.5 and *B* at 23 kHz) of ultrasonic cavitation in xenon saturated phosphoric acid, where an extremely bright SL emission occurs [23,24]. Experimental details, SL overview images, and movie sequences are contained in the Supplemental Material [25]. In accordance to other experiments with xenon in phosphoric or sulfuric acid [26,27], we measure SL flash widths in the range of 20 ns or less [25]. This is much shorter than all used camera exposure times (>1.9 μs), and thus typically no flash is distributed over more than one frame within a movie. For exposure times longer than an acoustic cycle, multiple flashes from one bubble can occur on an image. Since the sensor sensitivity does not depend on frame rate, the registered photons of an SL emission are essentially independent of the camera speed. We estimate the detection threshold for an SL flash in front of a low background light to range within 10^5–10^6 photons [25], and frequently we encounter pixel saturation from SL. On the other hand, it cannot be judged if "dark" recorded bubbles do not emit at all or just stay below this value.

Figure 1 shows examples of typical recording frames taken at different speeds. Since bubbles in a multibubble environment are usually moving in space [22], the light from repetitively flashing bubbles appears as a streak or chain of spots on longer-term exposures. Light emission

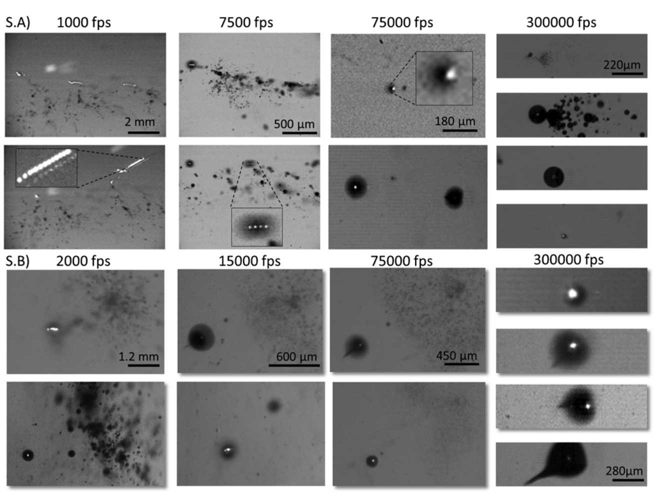

FIG. 1. Sample images from high-speed recordings at different frame rates and magnifications. Top: setup *A*, 36.5 kHz; large emitting bubbles run from right to left in a streamer, often followed by a "flock" of smaller bubbles. Bottom: setup *B*, 23 kHz; large emitting bubbles run partly back and forth in the vicinity of a dense bubble cloud closer to the ultrasound emitter. SL can occur together with pronounced jetting (indicated by an elongated bulge during bubble reexpansion). See also Supplemental Material videos [25].

happens always in the ultimate collapse peak, i.e., when the bubble volume is smallest. This is visible on the images only at the highest frame rates, otherwise the fast collapse and rebound bubble wall motion during exposure causes shadows of the bubble silhouette before and after collapse. From the shadows, important information like maximum bubble sizes and shapes can often nevertheless be obtained.

The evaluation of a large amount of high-speed sequences yields the following main results: (i) All observed extremely bright emitters of xenon in phosphoric acid are among the largest bubbles in the field, and emission strength basically increases with bubble size. Based on visual inspection, the maximum expansion radii $R_{\max}$ reach about 50 to 80 μm at 36.5 kHz and 75 to 240 μm at 23 kHz. Only few such large and emitting bubbles occur in the imaged bubble fields. We estimate their frequency of occurrence to about 1%–10% of the observable bubbles, where it has to be noted that the bubble number density generally increases towards smaller (nonemitting) bubble sizes (Supplemental Material, part I [25]). Here we define an emitting bubble as flashing at least once during the observation time. The largest bubbles within a group also show the fastest translation velocities (of the order of 0.5 to 2 m/s). (ii) Many emitting bubbles are flashing every oscillation cycle, i.e., the number of bright spots on a line of a moving bubble corresponds to the number of acoustic periods during exposure (insets in Fig. 1). As well, higher periods, modulated brightness, or erratic flashing have been observed. (iii) Bright SL appears to start after bubble growth to a critical size by coalescence processes. Further mergers can amplify the emission [Fig. 2(a)]. Flashing can end after bubble splitting induced by instabilities, triggered spontaneously after reaching a certain region in the cuvette, or by further collisions [Figs. 2(b)–(d)]. If emission begins (or is boosted) after a bubble growth by coalescence, flashing sets in rapidly [or immediately continues, Fig. 2(e)]. Usually no larger dark transient oscillations are observed after merging if the bubble stays stable. (iv) When expanded, the shape of the flashing bubbles always appears quite spherical (apart from collision events). However, many fast moving bubbles show jetting, i.e., a liquid jet traverses the collapsing bubble in translation direction and hits the opposing bubble wall. The jet is caused by conservation of added mass momentum if the initial bubble velocity is sufficiently high and/or the collapsed volume is very small [28–31]. Jetting bubbles can flash similar to spherical ones, but the brightness decreases when the jet becomes larger, ultimately leading to no detectable signal. This can be well observed for bubbles undergoing oscillatory spatial motion near the sound emitter in setup *B*, see Fig. 3: Here the radial expansion suddenly grows (probably due to a hysteresis [32]), and the direction of translational motion is reversed. The bubble accelerates, and the jet strength increases every collapse. At the same time, the recorded SL brightness diminishes until the

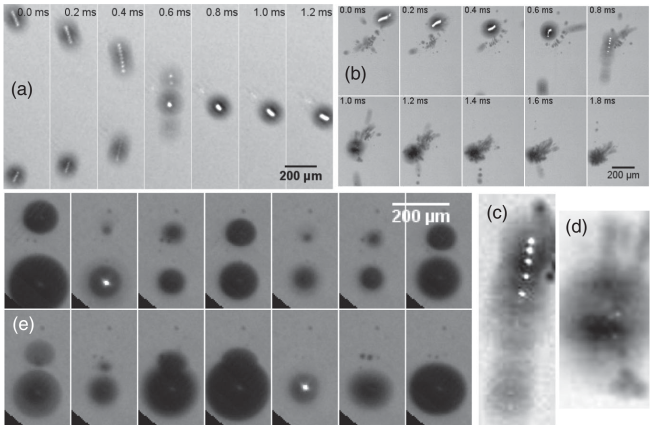

FIG. 2. Different collision scenarios of SL bubbles. (a) Similarly sized emitting bubbles merge and flash brighter (36.5 kHz, 5000 frames/ sec). (b) An SL bubble in a swarm of smaller bubbles merges with a similarly sized neighbor, becomes shape unstable, and disintegrates. The emission ceases (36.5 kHz, 5000 frames/ sec). (c),(d) Enlargements of the collision process from (b) at 0.8 and 1.0 ms [frame width in (c): 125 μm, in (d): 137 μm]. (e) A larger SL bubble shows emission directly in the first collapse after a merger with a smaller bubble (23 kHz, 75 000 frames/ sec, frame-to-frame time 13.3 μs). Images are processed for better printing.

detection threshold is reached (see Supplemental Material [25] for a quantitative evaluation of jetting and SL).

Since the dynamics in multibubble fields are in general not stationary, a closer analysis by light scattering [3,13,26] or stroboscopic imaging is very limited, and direct imaging with highest frame rates is desirable to obtain detailed histories of bubble sizes, shapes, and motions. Here we present the analysis of a transient bubble dynamics with SL, recorded with 525 000 frames/ sec (Fig. 4). The bubble in setup B shows the transition from an aperiodic (almost period-5) bubble oscillation towards a period-1 dynamics with expanded maximum radius (similar to the transition shown in Fig. 3). Some first collapses from the larger expansion result in extremely bright emission, while light from later bubble implosions ceases and cannot be detected (apparently due to pronounced jetting). The data are sufficient to estimate the conditions in the first emitting

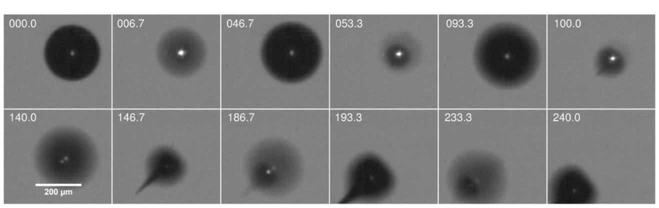

FIG. 3. Collapse events and light emissions of an accelerating large bubble that develops jetting (23 kHz, 150 000 frames/ sec, timing given in μs, frame width 470 μm). For each collapse, two subsequent frames are shown (full data in the Supplemental Material [25]).

collapse near 220 μs on the basis of a spherical bubble model fit [26,33,34]. We use a Keller-Miksis model for radial dynamics coupled to translational motion of the bubble [31]. Heat conduction is approximately incorporated by a variable polytropic exponent, and the temperature dependence of the heat conductivity of xenon is included (see Supplemental Material, part II for full model details [25]). The model predicts a volume compression ratio of 227 and a peak temperature around 38 000 K. Since potential jetting, phase transitions, and chemical reactions are neglected, the values obtained will be overestimated. Still, an extended model considering water chemistry has been reported to yield similar temperature values for SBSL conditions [35], where the energy losses due to chemical

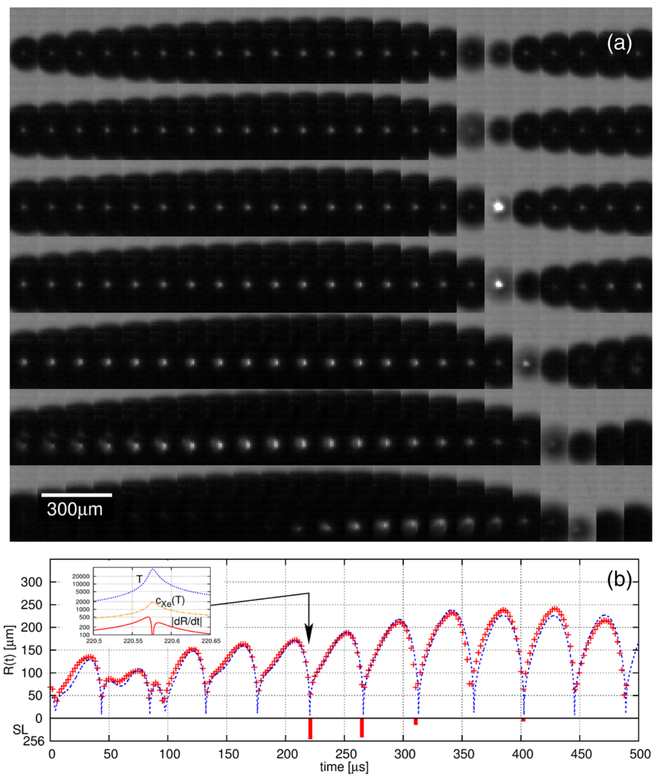

FIG. 4. Observation of a transient bubble oscillation with extremely bright emission (23 kHz, 525 000 frames/ sec). (a) Part of the high-speed recording presented as collocated stripes, time proceeds linewise from top to bottom (scale indicated). (b) Radius-time data (red crosses) and numerical fit (dashed blue line) with pressure amplitude $p_a = 184.6$ kPa and equilibrium bubble radius $R_0 = 36.7$ μm, which reproduce the peculiar aperiodic bubble oscillation quite well [see also Supplemental Material, part II]. Maximum pixel readouts of the identified SL flashes are depicted as negative-going red bars below the zero line. The frames shown correspond to the time interval between 100 and 406 μs. For the strongest SL signal around 220 μs, the inset shows the model results for temperature T [K], bubble wall speed $|dR/dt|$ [m/s], and sound speed in the heated xenon gas $c_{\mathrm{Xe}(T)}$ [m/s]. Since jetting, evaporation or condensation and chemistry are not included in the model, the values are supposed to be upper bounds.

reactions of water remained small. We further note that for our case, the calculated bubble wall motion reaches inward velocities beyond 500 m/s, but does not exceed the actual sound speed of xenon [increasing with the square root of gas temperature; see inset of Fig. 4(b)]. This might cast an internal shock wave into doubt.

In comparison to SBSL in acids [13,26,33], MBSL bubbles show some dynamical analogies, e.g., roughly similar volume compression ratios, or higher periodic oscillations with intermittent SL activity. However, significant differences to SBSL occur due to spatial translation, interaction and collision of bubbles with each other, which leads to transient SL bubble dynamics (i.e., not necessarily positionally, diffusionally, and mostly shape stable bubble conditions like in SBSL). This allows for partly larger (although unstable and potentially aspherical) emitting bubbles in the MBSL systems, facilitated by higher dissolved gas content in the liquid and rapid growth by bubble collisions and merging. Most importantly, MBSL emissions originate to a good part from nonspherical geometries, especially from clearly jetting bubbles. Frequently the jetting is observed to be induced by fast translational motion [20,31] (similar behavior is to be expected for moving SBSL bubbles [13,17,18], but has not been documented yet). Although we observe extreme liquid jets to diminish and extinct detectable SL emissions, it has to be emphasized that moderate jetting is well compatible with SL, and a spherical collapse peak is not a prerequisite for sufficient energy focusing for bright luminescence (compare also Refs. [9,36,37]). The same holds for bubbles located close to neighbor bubbles or within a bubble group where interactions will lead to nonspherical collapse deformations. This appears tolerable for SL to some degree, which is seen, for instance, in the example of immediate flashing after bubble merging, Fig. 2(e). We like to note that a certain insensitivity to bubble deformations is also assumed for SBSL systems, e.g., with respect to gravity induced pressure gradients [38] or to saturated shape instabilities [39]. In our study, the only necessary condition we observe for SL emission is a sufficiently large maximum bubble size. Our observations suggest that indeed the jetting collapse modality is generic for a good part of bubbles in a multibubble field, including luminescing ones. Additionally, this supports the droplet injection scenario [19] based on jetting [20] as a promoter of excitation and chemistry of nonvolatile species in collapsing bubbles. Consequently, the findings show a clear motivation for further development and application of advanced models for nonspherical and jetting bubble geometries including heat and mass transfer. This goes beyond the spherical modeling employed here and is a challenging task (see, e.g., Ref. [40]).

In conclusion, we have demonstrated the simultaneous high-speed imaging of cavitation bubble dynamics and individual MBSL emissions in xenon sparged phosphoric acid. The method allows for a unique observation of the conditions in multibubble environments that lead to the extreme energy focusing in a bubble collapse. Such data on realistic collapse modalities are necessary for an advanced description of the bubble interior by extended, in particular nonspherical models. Moreover, the knowledge of active bubble distributions in multibubble fields appears mandatory for substantial improvements of many applications of acoustic cavitation, notably of sonochemistry. Future investigations certainly will employ even more sensitive high-speed imaging devices, reducing the flash detection threshold. Following this line, a more complete direct mapping of MBSL activity and photometry of individual bubbles should be possible, also for other gas-liquid systems.

The financial support by the Austrian Federal Ministry of Science, Research and Economy and the National Foundation for Research, Technology and Development is gratefully acknowledged.

*Corresponding author.
robert.mettin@phys.uni-goettingen.de

[1] H. Frenzel and H. Schultes, Z. Phys. Chem. B **27**, 421 (1935).
[2] F. O. Schmitt, C. H. Johnson, and A. R. Olson, J. Am. Chem. Soc. **51**, 370 (1929).
[3] S. Putterman and K. Weninger, Annu. Rev. Fluid Mech. **32**, 445 (2000).
[4] F. R. Young, *Sonoluminescence* (CRC Press, Boca Raton, 2004).
[5] K. S. Suslick, Science **247**, 1439 (1990).
[6] T. J. Mason and J. P. Lorimer, *Applied Sonochemistry* (Wiley-VCH, Weinheim, 2002).
[7] T. G. Leighton, *The Acoustic Bubble* (Academic, London, 1994).
[8] A. A. Buzukov and V. S. Teslenko, Sov. Phys. JETP Lett. **14**, 189 (1971).
[9] C. D. Ohl, O. Lindau, and W. Lauterborn, Phys. Rev. Lett. **80**, 393 (1998).
[10] O. Baghdassarian, B. Tabbert, and G. A. Williams, Phys. Rev. Lett. **83**, 2437 (1999).
[11] D. F. Gaitan, L. A. Crum, C. C. Church, and R. A. Roy, J. Acoust. Soc. Am. **91**, 3166 (1992).
[12] B. P. Barber, R. A. Hiller, R. Löfstedt, S. J. Putterman, and K. R. Weninger, Phys. Rep. **281**, 65 (1997).
[13] R. Urteaga and F. J. Bonetto, Phys. Rev. Lett. **100**, 074302 (2008).
[14] T. J. Matula, R. A. Roy, P. D. Mourad, W. B. McNamara, and K. S. Suslick, Phys. Rev. Lett. **75**, 2602 (1995).
[15] K. J. Taylor and P. D. Jarman, Aust. J. Phys. **23**, 319 (1970).
[16] C. Cairós, J. Schneider, R. Pflieger, and R. Mettin, Ultrason. Sonochem. **21**, 2044 (2014).
[17] D. J. Flannigan and K. S. Suslick, Nature (London) **434**, 52 (2005).
[18] D. J. Flannigan and K. S. Suslick, Phys. Rev. Lett. **99**, 134301 (2007).

[19] H. Xu, N. C. Eddingsaas, and K. S. Suslick, J. Am. Chem. Soc. **131**, 6060 (2009).

[20] A. Thiemann, F. Holsteyns, C. Cairós, and R. Mettin, Ultrason. Sonochem. **34**, 663 (2017).

[21] T. G. Leighton, Ultrason. Sonochem. **2**, S123 (1995).

[22] R. Mettin, in *Bubble and Particle Dynamics in Acoustic Fields: Modern Trends and Applications*, edited by A. A. Doinikov (Research Signpost, Kerala, 2005), p. 1.

[23] A. Chakravarty, T. Georghiou, T. E. Phillipson, and A. J. Walton, Phys. Rev. E **69**, 066317 (2004).

[24] K. S. Suslick, N. C. Eddingsaas, D. J. Flannigan, S. D. Hopkins, and H. Xu, Ultrason. Sonochem. **18**, 842 (2011).

[25] See Supplemental Material at http://link.aps.org/supplemental/10.1103/PhysRevLett.118.064301 for part I: Notes on experimental details, bubble size distributions, SL emission spectra, estimates of SL recording sensitivity, more data and images on jetting and SL. Part II: Details of numerical model. Videos A and B: Movie material to setups *A* and *B*.

[26] S. D. Hopkins, S. J. Putterman, B. A. Kappus, K. S. Suslick, and C. G. Camara, Phys. Rev. Lett. **95**, 254301 (2005).

[27] C. Lim, J.-S. Jeong, and H.-Y. Kwak, Europhys. Lett. **86**, 17002 (2009).

[28] T. B. Benjamin and A. T. Ellis, Phil. Trans. R. Soc. A **260**, 221 (1966).

[29] J. R. Blake, G. S. Keen, R. P. Tong, and M. Wilson, Phil. Trans. R. Soc. A **357**, 251 (1999).

[30] Q. X. Wang and J. R. Blake, J. Fluid Mech. **659**, 191 (2010).

[31] T. Nowak and R. Mettin, Phys. Rev. E **90**, 033016 (2014).

[32] R. Mettin and A. A. Doinikov, Appl. Acoust. **70**, 1330 (2009).

[33] D. J. Flannigan, S. D. Hopkins, C. G. Camara, S. J. Putterman, and K. S. Suslick, Phys. Rev. Lett. **96**, 204301 (2006).

[34] S. Hilgenfeldt, S. Grossmann, and D. Lohse, Phys. Fluids **11**, 1318 (1999).

[35] A. Moshaii, M. Faraji, and S. Tajik-Nezhad, Ultrason. Sonochem. **18**, 1148 (2011).

[36] O. Baghdassarian, H. C. Chu, B. Tabbert, and G. A. Williams, Phys. Rev. Lett. **86**, 4934 (2001).

[37] B. Kappus, S. Khalid, and S. Putterman, Phys. Rev. E **83**, 056304 (2011).

[38] M. S. Longuet-Higgins, Proc. R. Soc. A **453**, 1551 (1997).

[39] M. Levinsen, Phys. Rev. E **90**, 013026 (2014).

[40] A. J. Szeri, B. D. Storey, A. Pearson, and J. R. Blake, Phys. Fluids **15**, 2576 (2003).